Surface Functionalization

International Edition: DOI: 10.1002/anie.201604973
German Edition: DOI: 10.1002/ange.201604973

Site-Targeted Interfacial Solid-Phase Chemistry: Surface Functionalization of Organic Monolayers via Chemical Transformations Locally Induced at the Boundary between Two Solids

Rivka Maoz, Doron Burshtain, Hagai Cohen, Peter Nelson, Jonathan Berson, Alexander Yoffe, and Jacob Sagiv**

Abstract: *Effective control of chemistry at interfaces is of fundamental importance for the advancement of methods of surface functionalization and patterning that are at the basis of many scientific and technological applications. A conceptually new type of interfacial chemical transformations has been discovered, confined to the contact surface between two solid materials, which may be induced by exposure to X-rays, electrons or UV light, or by the application of electrical bias. One of the reacting solids is a removable thin film coating that acts as a reagent/catalyst in the chemical modification of the solid surface on which it is applied. Given the diversity of thin film coatings that may be used as solid reagents/catalysts and the lateral confinement options provided by the use of irradiation masks, conductive AFM probes or stamps, and electron beams in such solid-phase reactions, this approach is suitable for precise targeting of different desired chemical modifications to predefined surface sites spanning the macro- to nanoscale.*

Recent exploratory experiments conducted by us with the purpose of devising a comprehensive methodology of surface chemical functionalization and patterning led to the rather surprising discovery that the top CH_3 groups of highly ordered OTS monolayers (monolayers self-assembled from *n*-octadecyltrichlorosilane precursor molecules, $SiCl_3$–$(CH_2)_{17}$–CH_3)[1,2] may be quantitatively converted to COOH with full preservation of the composition and structure of the monolayer hydrocarbon core using various thin-film coatings as oxidizing reagents. The conversion of OTS into OTSox (surface-oxidized OTS) is implemented upon exposure of the coated OTS monolayer to different sources of electromagnetic radiation or electrons (see Scheme 1 for some representative examples). Reaction route (a) in Scheme 1 was discovered by accident in experiments involving electron beam (e-beam) deposition of different metals (Ag, Al, Au, Ti) on OTS monolayers on silicon (OTS/Si) or quartz (OTS/Q) covered with 4–10 nm-thick PVA (polyvinyl alcohol) film coatings. Depositing the same metals (under identical experimental conditions) on bare OTS monolayers did not affect their composition and structure in any measurable manner, whereas using a tungsten target in the e-beam evaporator operated under conditions below the threshold evaporation of this metal was found to convert OTS into OTSox as in the actual deposition of metals on the PVA surface. Finally, using thermal instead of e-beam metal deposition on PVA-coated OTS monolayers did not affect their composition and structure either. These observations suggested that, in the presence of a source of oxygen (here the thin PVA coating), the surface oxidation of OTS is induced by the radiation that accompanies the metal evaporation in e-beam evaporators (X-rays, secondary and scattered electrons and UV light, emitted when energetic electrons strike a metal target)[3] rather than by the metal deposition itself. That each of the different components of this radiation may induce the conversion of OTS to OTSox was confirmed by carrying out separate irradiation experiments with X-rays from the source

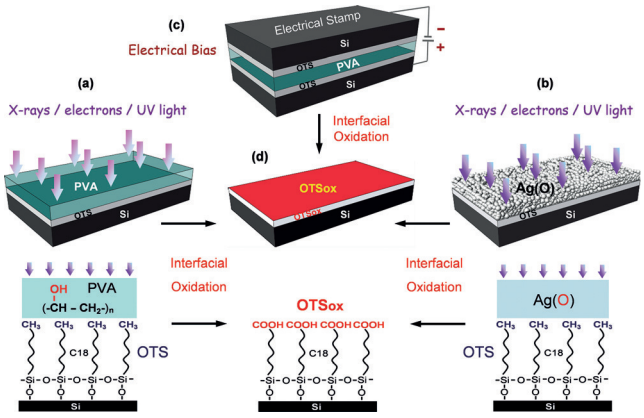

Scheme 1. Interfacial solid-phase oxidation of OTS/Si monolayer to OTSox/Si using thin PVA or oxide-covered silver [Ag(O)] films as oxidation reagents (see text): a)–c) Examples of different large-area reaction set-ups and corresponding molecular structures (representation not to scale). d) The bare OTSox surface is revealed upon removal of the respective thin film coatings (being a), c) PVA or b) Ag(O)) following completion of the oxidation process.

[*] Dr. R. Maoz, Dr. D. Burshtain, Dr. P. Nelson, Dr. J. Berson, Prof. J. Sagiv
Department of Materials and Interfaces
Weizmann Institute of Science, Rehovot 76100 (Israel)
E-mail: rivka.maoz@weizmann.ac.il
jacob.sagiv@weizmann.ac.il
Dr. H. Cohen, A. Yoffe
Department of Chemical Research Support
Weizmann Institute of Science, Rehovot 76100 (Israel)
Dr. J. Berson
Present address: Institute of Nanotechnology and Institute of Applied Physics, Karlsruhe Institute of Technology (KIT)
76128 Karlsruhe (Germany)

Supporting information and the ORCID identification number(s) for the author(s) of this article can be found under: http://dx.doi.org/10.1002/anie.201604973.

of an X-ray photoelectron spectrometer (XPS), electrons emitted by the electron flood gun of the same instrument, electrons from an e-beam lithography system, and light emitted by UV lamps. These results led to the initiation of a research program aiming at a basic investigation as well as possible applications of such solid–solid interfacial chemical transformations. Interesting novel findings obtained to date point to 1) the possible introduction of different functional groups by the use of different organic or inorganic thin film coatings as solid reagents/catalysts, for example, PVA or oxide-covered silver (Ag(O) in Scheme 1 b, formed by the exposure of thin silver films to air) for carboxylation, AgCl for chlorination, and gelatin for amination, and 2) the possible use of either electron beams or electrons injected into the thin film coating by means of conductive AFM (atomic force microscope) probes or stamps as versatile tools of local surface functionalization and patterning. AFM and electrical stamp setups suitable for this purpose (in Scheme 1 c, a bare OTS/Si specimen is used as stamp) differ from those previously employed in the local electrochemical functionalization and patterning of OTS/Si monolayers by constructive lithography (CL)[4–6] in that here a dry solid film replaces the interfacial water layer that was shown to play a key role as oxidant in the different variants of the CL[4,5] and related local oxidation lithographic processes[7] reported to date. The possible use of solid coatings as interfacial thin film reagents instead of water paves the way to an entire new area of research, with applications that in principle are not feasible with volatile liquid layers.

Herein we report proof-of-concept experimental results demonstrating large-area surface functionalization and micropatterning of OTS/Si monolayers via several different routes of interfacial solid-phase oxidation (Scheme 1, Figure 1, Figure 3) and interfacial solid-phase chlorination induced by UV irradiation of AgCl thin film coatings (Figure 2, Figure 3). Exploratory experiments reported in the Supporting Information further demonstrate the possible introduction of amino functionality on the top OTS surface as well as the implementation of a reverse oxidation process whereby thin films of a long *n*-alkane or PVA deposited on bare silicon oxide are oxidized upon exposure to UV light, the underlying surface oxide being thus reduced in this interfacial reaction. Surface patterns were also generated in the PVA/silicon oxide system using irradiation masks (Supporting Information). These results point to the wide scope of such interfacial solid-phase chemical transformations, beyond the functionalization and patterning of organic monolayers. The well-defined OTS/Si system, however, offers an ideally suited experimental platform for basic investigations of chemistry at interfaces, besides presenting particular interest by itself as an inherently patternable single-layer functional material that displays unusual electrical conduction properties.[6] Results obtained in the advancement of a surface nanopatterning method based on solid-phase chemical processes of this kind will be reported in separate publications. Future publications will also address mechanistic aspects of these processes along with a discussion of reaction conditions affording a particular surface transformation.

Evidence for the selective oxidation of the top CH_3 groups of OTS/Si monolayers to COOH via reaction route (a) in Scheme 1 using two different sources of radiation (under conditions that do not affect the monolayer core) is presented in Figure 1 (see also the Supporting Information, Figures S1–S3). The FTIR spectra in Figure 1 a were acquired from an OTS/Si specimen covered with a 4–6 nm-thick dry PVA film (Supporting Information, Figures S1, S2) before and after its exposure for 5 seconds to the mixed radiation emitted in an e-beam evaporator[3] from a tungsten target in the absence of detectable metal deposition (W irradiation). For comparison, spectra of the as-prepared OTS/Si monolayer and the reacted monolayer after complete removal of the irradiated PVA coating are also included in Figure 1 a, a detailed view of same

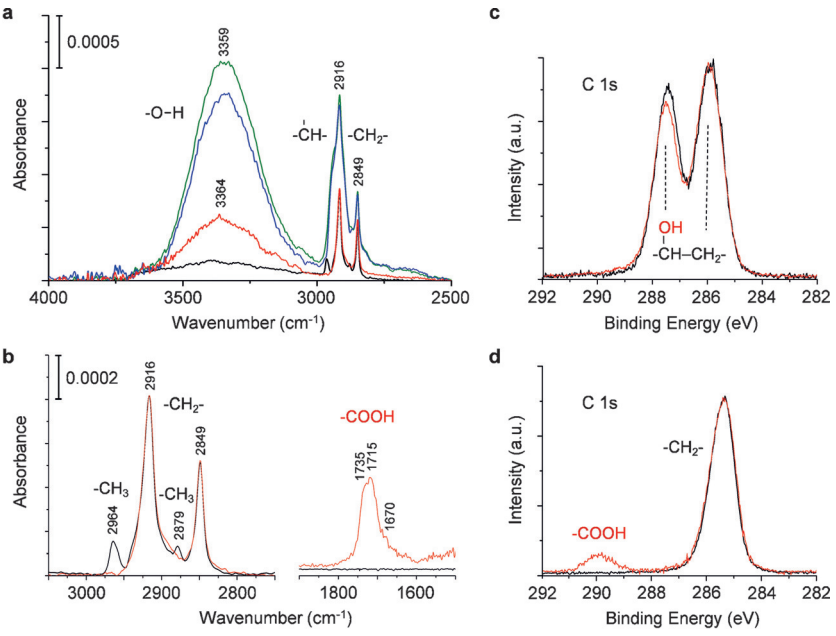

Figure 1. a), b) Quantitative Brewster's angle FTIR spectra[9,6] of a pristine OTS/Si monolayer (black trace), same specimen coated with a thin PVA film (green trace), the PVA-coated monolayer after its W irradiation in an e-beam evaporator (blue trace), the irradiated monolayer after removal of the PVA film (red trace). c) XPS spectra (0° emission angle) of a PVA-coated OTS/Si monolayer specimen like that in (a), before (black trace) and after (red trace) its X-ray irradiation in an XPS instrument. d) XPS spectra (0° emission angle) of the irradiated monolayer in (c), recorded after complete removal of the irradiated PVA film (red trace), and of the pristine OTS/Si monolayer before the deposition of the PVA film (black trace). To facilitate a comparison of the relative intensities of the different C 1s lines, the XPS curves were normalized by adjusting their CH_2 peak intensities to the same arbitrary value. Because exposure to low energy electrons may induce similar interfacial chemical transformations, all XPS spectra in this study were obtained without the use of an electron flood gun for charge neutralization, and so may display variable peak shifts caused by surface charging.

spectra over a different spectral range being presented in Figure 1 b. The disappearance, following irradiation, of the methyl C–H stretch vibrations at 2964 cm^{-1} (antisymmetric) and 2879 cm^{-1} (symmetric) (Figure 1 a,b), accompanied by the appearance of characteristic C=O stretch modes of the carboxylic acid around 1715 cm^{-1} (hydrogen-bonded oligomeric species at 1670 cm^{-1}, dimers at 1715 cm^{-1}, and monomeric acid at 1735 cm^{-1}) (Figure 1 b),[6,8] and the broad O–H stretch mode of COOH centered at 3364 cm^{-1} (Figure 1 a),[6] bear evidence for the quantitative conversion of the CH_3 groups of OTS to COOH. This surface transformation occurs with virtually no change in the intensities, positions and widths of the methylene H–C–H stretch bands at 2916 cm^{-1} (antisymmetric) and 2849 cm^{-1} (symmetric; Figure 1 a,b), which are characteristic of alkyl tails in their fully extended all-*trans* conformation adopted in densely packed monolayers.[1b–d,9] Thus, the conversion of OTS into OTSox was achieved with full preservation of the composition and structure of the hydrocarbon core of the monolayer. The irradiation is further seen to cause a significant drop in the intensity of the broad band centered at 3359 cm^{-1} (Figure 1 a). This band combines the O–H stretch modes of hydrogen-bonded PVA hydroxyls and OTS silanols (before irradiation), and PVA O–H species and OTSox carboxyl and silanol groups (after irradiation). A comparison of the different curves in this spectral region indicates that the major contribution to this band comes from the PVA hydroxyl groups (Figure 1 a; Supporting Information, Figure S2). Thus, the drop in its intensity, accompanied by a much smaller decrease in the intensities of the PVA C–H stretch modes that overlap with those of OTS or OTSox at 2916 cm^{-1} and 2849 cm^{-1} (Supporting Information, Figure S2), points to radiation-induced changes in the PVA film associated with loss of OH groups.[10] This observation is consistent with the notion that the oxy species involved in the surface oxidation of the OTS monolayer originate in PVA hydroxyl groups that are consumed upon irradiation.[10,11] XPS data offer further support to this view.

The XPS spectra in Figure 1 c, collected from a similar PVA/OTS/Si specimen before and after its exposure to the monochromatic X-ray beam of the spectrometer for 1–2 hours (see the Experimental Section), show a significant drop following irradiation in the C 1s line ascribed to the CHOH moieties of PVA relative to that ascribed to CH_2. Like the IR data in Figure 1 a, this points to loss of PVA hydroxyl groups.[10] The contribution of OTS or OTSox alkyl tails to this CH_2 line is rather weak because of the attenuation of photoelectrons ejected from any deep location under the PVA film. XPS spectra of the pristine OTS monolayer and the bare OTSox monolayer (acquired after complete removal of the irradiated PVA coating) are displayed in Figure 1 d. Consistent with the position of the -COOH functions at the outer monolayer surface and the depth attenuation of the XPS signals,[1d] the elemental ratio COOH/CH_2 of about 1:12 obtained from the respective C 1s signals recorded after irradiation is indeed considerably higher than their stoichiometric ratio (1:17) in the OTSox molecule.[1d] This interfacial oxidation process is thus selective, affecting only the outer methyl groups of the OTS monolayer. IR spectra recorded before and after the X-ray–induced conversion of OTS into OTSox (Supporting Information, Figure S3) are virtually identical to those recorded from the W-irradiated specimen displayed in Figure 1 b. This confirms that the monochromatic X-ray radiation and the mixed radiation in the e-beam evaporator induce essentially the same interfacial transformation. Likewise, the same interfacial transformation could also be induced by the exposure of PVA/OTS/Si specimens to UV radiation ($\lambda = 185$ nm, 10 min) under argon (see the Experimental Section). To check that COOH is the only carbonyl species present on the surface of the final OTSox products, IR spectra were recorded also from OTSox/Si specimens following their treatment with an aqueous solution of silver acetate, which converts the carboxylic acid monolayer surface into the corresponding silver carboxylate salt.[6] As shown in the Supporting Information, Figure S3, this treatment indeed results in the disappearance of all COOH spectral features around 1715 cm^{-1} along with the concomitant appearance of the characteristic antisymmetric and symmetric COO^-Ag^+ carboxylate stretch modes at 1530 cm^{-1} and 1406 cm^{-1}, respectively.[6]

Interfacial chlorination experiments were performed by UV irradiation ($\lambda = 300$ nm) under argon of OTS/Si monolayers coated with 10–50 nm thick oxide-covered silver films

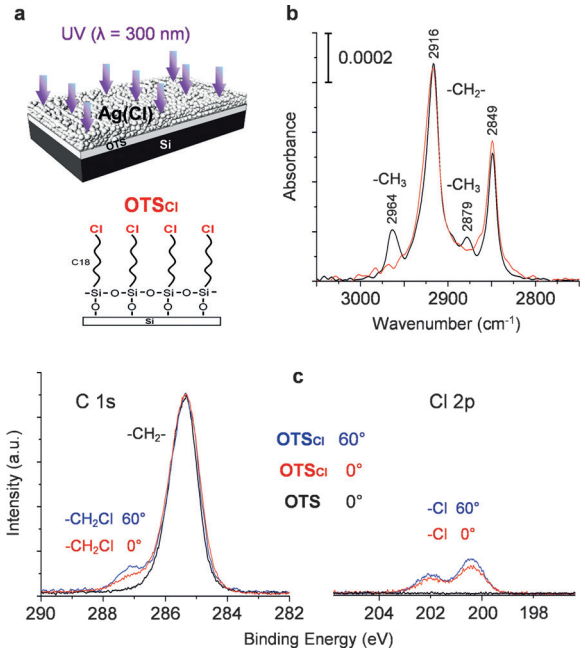

Figure 2. Interfacial solid-phase chlorination of OTS/Si monolayer using a thin Ag(Cl) film as reagent (see text): a) Reaction set-up and the molecular structure of the reacted monolayer, OTS_{Cl}/Si (representation as in Scheme 1). b) FTIR spectra (as in Figure 1 b) of a pristine OTS/Si monolayer (black trace) and same monolayer after 30 min UV irradiation through a ca. 50 nm-thick Ag(Cl) film and its subsequent dissolution (OTS_{Cl}/Si, red trace). c) XPS spectra of a pristine OTS/Si monolayer (black trace, 0° emission angle) and the OTS_{Cl}/Si monolayer at 0° (red trace) and 60° (blue trace) emission angles. To facilitate a direct comparison of the relative angle-dependent intensities of the Cl (Cl 2p) and CH_2Cl (C 1s) lines, all curves were normalized by adjusting the respective CH_2 (C 1s) peak intensities to the same arbitrary value.

that were converted in situ into AgCl by exposure for several minutes to HCl vapors[12] in a closed vessel above concentrated (37%) aqueous HCl (Ag(Cl); Figure 2a). Evidence for the selective chlorination of the top OTS surface, resulting in the quantitative conversion of CH_3 to CH_2Cl moieties in the reacted monolayer (OTS_{Cl}), is provided by the combined analysis of the FTIR and XPS spectra in Figure 2. As in Figure 1b, the disappearance of the methyl and preservation of the methylene spectral features following irradiation (Figure 2b) is indicative of a selective surface transformation that affects the outer CH_3 groups of the OTS monolayer only, its initial highly ordered structure remaining unaffected. The XPS curves in Figure 2c confirm the quantitative conversion of CH_3 to CH_2Cl moieties. Thus, both the elemental ratios CH_2Cl carbon/total carbon and Cl/total carbon (circa 1:13 at 0° emission angle) and the higher relative CH_2Cl (C 1s) and Cl 2p signals at 60° emission angle (by a factor of ca. 1.17) are theoretically consistent with the presence of a CH_2Cl moiety at the outer end of each C18 alkyl tail of the reacted monolayer. The selective chlorination of surface exposed methyls achieved in this interfacial reaction is particularly remarkable in view of the higher intrinsic reactivity of CH_2 compared to CH_3 in the photochlorination of alkanes in bulk fluid phases.

Effective lateral confinement of the oxidation and chlorination reactions to predefined surface sites of micrometric dimensions was achieved by means of simple contact masks or patterned electrical stamps (e-stamps) pressed against the thin film-coatings of the respective monolayer specimens during their irradiation (variants of the set-ups in Scheme 1a,b and Figure 2a) or the application of electrical bias (variants of the set-up in Scheme 1c). Examples of monolayer patterns fabricated in this manner, consisting of arrays of OTSox/Si or OTS_{Cl}/Si dots or squares surrounded by the unmodified OTS/Si monolayer (denoted OTSox@OTS/Si and OTS_{Cl}@OTS/Si, respectively), are shown in Figure 3. TEM (transmission electron microscope) grids were used here as contact masks for both irradiation and the preparation of patterned metal-on-monolayer e-stamps.[5b] It should be noted that practically identical results were obtained with e-beam evaporator irradiation accompanied by metal deposition (for example Figure 3a,b) or metal-free W irradiation (Figure 1a,b). All patterned features in Figure 3 are faithful reproductions of the hole and bar features of the respective TEM grids used as masks. The contrast in these lateral force images between reacted and unmodified surface regions points to a considerably higher friction within the former.[4–6] This is consistent with the higher polarity of the outer surface of both OTSox and OTS_{Cl} compared to that of OTS. The inverted contrast in simultaneously acquired contact mode topographic (height) and lateral force (friction) images along with its inversion in both images as the tip motion in the horizontal scan changes direction, and the absence of significant height difference between modified and unmodified surface regions in the respective semicontact topographic images (Supporting Information, Figure S4) are characteristic features of constructive lithography.[4b–d,5b,6] Consistent with the FTIR and XPS data discussed above, these findings thus offer direct evidence for site-confined chemical modifications of the outer monolayer surface that do not affect its hydrocarbon core.

In summary, conclusive evidence was provided for both large-area (square centimeters) and analogous site-selected microscale surface chemical modifications of OTS/Si monolayers realized by a new type of interfacial chemical processes that may be induced at the boundary between the monolayer and a reactive thin film coating upon exposure to various sources of electromagnetic radiation or electrons. Such processes offer remarkable versatility in the fabrication of top-functionalized monolayers and chemically patterned monolayer surfaces starting with an inert, densely packed monolayer assembled from the simplest commercial organosilane. Thus, apart from yielding the highest possible surface density of the installed functionality, this in situ approach also circumvents the need of investing expensive and time-consuming efforts in the synthesis of functional monolayer-forming precursors. Novel catalytic aspects of the interfacial chemical transformations reported here are evident in the utilization of Ag(O) and Ag(Cl) films as solid carriers of reactive oxygen or chlorine that can be regenerated upon their simple exposure to, respectively air and air + HCl vapors.[14] These findings pave the way to the advancement of a generic methodology of surface functionalization and patterning based on the possible targeting of different solid-phase chemical modifications of this kind to predefined surface sites. Depending on the selected mode of implementation, this method is compatible with either or both conductive and insulating materials. Future publications will report applications to surface nanopatterning with focused

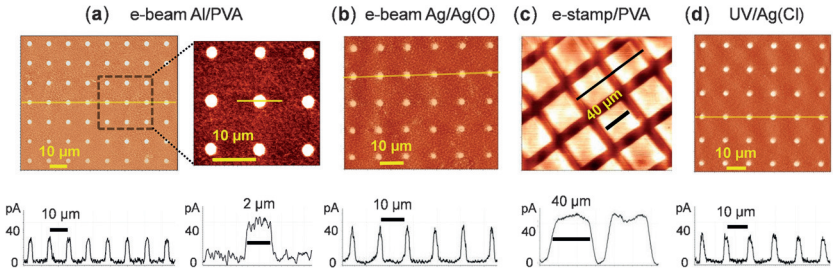

Figure 3. Examples of AFM images (lateral force, contact mode) of monolayer micropatterns fabricated by variants of the interfacial solid-phase oxidation and chlorination processes depicted in Scheme 1 and Figure 2a, respectively: a) OTSox@OTS/Si dots pattern produced by e-beam deposition of ca. 30 nm of aluminum through a TEM grid contact mask on a PVA(ca. 7 nm)/OTS/Si specimen (Scheme 1, route a). b) Dots pattern as in (a) produced by e-beam deposition of ca. 40 nm of silver through same contact mask on a OTS/Si monolayer coated with ca. 10 nm of oxide-covered silver (Scheme 1, route b). c) Squares pattern fabricated via route c in Scheme 1 on a PVA(ca. 4.5 nm)/OTS/Si specimen using an electrical stamp (consisting of an array of ca. 40 nm-thick silver squares deposited on a OTS/Si specimen through a TEM grid contact mask) to which a bias of −20 V was applied for 2 h.[13] d) OTS_{Cl}@OTS/Si dots pattern produced by 30 min UV irradiation through same TEM grid mask as in (a) and (b) of a OTS/Si monolayer coated with about 10 nm of Ag(Cl) (process depicted in Figure 2a). All AFM images were recorded after removal of the respective thin film coatings and metals further deposited in (a) and (b).

electron beams or electrical AFM probes as well as studies aiming at the optimization of such solid-phase processes of interest and the elucidation of their mechanisms.

Experimental Section

High-quality OTS monolayers were prepared on double-sided polished silicon wafer substrates (0.5 mm thick, *p*-type, ⟨100⟩, resistivity 8–11 Ω cm) covered with their native oxide layer using materials and procedures as described before.[5] PVA thin-film coatings were prepared by slow retraction of OTS/Si specimens from dilute aqueous solutions (0.1–0.2 %) of Mowiol 28–99 (Kuraray) at the room temperature (for details see the Supporting Information, Figures S1, S2). The PVA film was then removed from one side of the silicon wafer by Scotch-tape peeling. Because of the spontaneous formation of ester linkages between thin PVA coatings and the carboxylic acid surface moieties of OTSox monolayers, complete removal of the PVA from reacted monolayer (OTSox) surfaces was achieved by exposure to hydrolytic conditions (4–5 h in 5 % aqueous HCl at 70 °C) followed by slow cooling down to the ambient temperature, thorough overflow rinse with pure water and final blow off of water sticking to reacted portions of the surface with clean nitrogen withdrawn from liquid N_2. Evidence for the complete removal of PVA coatings was provided by FTIR spectra, AFM images, and XPS data collected from specimens repeatedly subjected to this hydrolytic treatment.

The e-beam deposition of thin metal films and the W irradiation were carried out in a 6 kW e-beam evaporator operated under conditions that do not cause damage to the bare or thin film-coated OTS/Si monolayers.[5b] Irradiated Ag(O) and Ag(Cl) coatings were removed from reacted specimens by dissolution in respectively 5 % aqueous HNO_3 and 5 % aqueous HNO_3 followed by 5 % aqueous HCl, thorough overflow rinse with pure water and final blow off of the water sticking to reacted portions of the surface with clean nitrogen withdrawn from liquid N_2. The absence of XPS Ag lines in specimens examined after exposure to these treatments along with AFM images collected from such specimens confirm the complete removal of these thin film coatings.

The X-ray irradiation was performed in the analysis chamber of a Kratos AXIS-Ultra DLD spectrometer equipped with a monochromatized Kα X-ray source (1486.6 eV, 75 W). To cover a surface area suitable for the collection of high quality Brewster's angle FTIR spectra (ca. 13 mm × 10 mm),[9] the irradiation was performed by serially exposing to the X-ray beam 128 discrete surface spots (each spot for 1 h), the centers of adjacent spots being 1 mm separated from one another. This procedure ensures overlap between neighboring irradiated spots (based on the intensity profile of the X-ray beam striking the sample surface), the effective irradiation time of the examined area at ca. half the nominal (75 W) power being estimated at 1–2 h.

XPS data were collected on the same Kratos spectrometer at 0° and 60° emission angles with respect to the surface normal without using the electron flood gun. The latter was found to induce interfacial chemical transformations like the X-ray radiation, which will be discussed elsewhere.

The UV irradiation ($\lambda_{max} = 300$ nm) was performed in a circular apparatus fitted with low-pressure mercury lamps. Specimens were placed in quartz containers continuously flushed with pure argon circa 2 h before as well as during the irradiation, at a distance of about 10 cm in front of the nearest UV lamp. The irradiation at $\lambda_{max} =$ 185 nm was performed in a UV cleaner apparatus equipped with Hg-vapor lamps (model NL-UV 253, NLE, Nagoya, Japan), under argon purge (Ar purity, 99.9999 %).[5a] As reported before,[5a] exposure of bare OTS/Si monolayers to such UV radiation results in photocleavege and removal of the alkyl tails from the surface.

The e-stamp surface modification and patterning was carried out using an electrical stamping device specially designed for this purpose[5] that was continuously flushed with dry nitrogen withdrawn from liquid N_2.

Quantitative Brewster's angle FTIR spectra (4 cm^{-1} resolution) were acquired as described before[9,5a,6] on a Bruker Equinox 55 spectrometer equipped with a liquid nitrogen-cooled MCT detector, a KRS-5 wire grid polarizer and a computer-controlled shuttle accessory, purged with dry nitrogen withdrawn from liquid N_2. Displayed spectral curves represent net spectra of the respective monolayers and PVA-coated monolayers on the front side of the double-side polished silicon wafer substrate, after subtraction of the spectral contributions of the bare silicon substrate (recorded before the deposition of the OTS monolayer) and of the unmodified OTS monolayer on its back side.

AFM images were acquired on an NTEGRA Aura System (NT-MDT) equipped with 100 μm or 200 μm (DualScan mode) scanners, purged with dry nitrogen withdrawn from liquid N_2 (3–5 % RH).[6] The contact mode imaging (Figure 3; Supporting Information, Figure S4) was carried out with Nanoworld Contr-50 silicon probes and the semicontact mode imaging (Supporting Information, Figure S4) with Bruker Tespa V2 silicon probes.

Acknowledgements

This research was supported by the Minerva Foundation with funding from the Federal German Ministry of Education and Research, the G. M. J. Schmidt Minerva Center of Supramolecular Architectures, and the Israel Science Foundation (grant No. 931/12). We are grateful to Omri Westmark for assistance with the graphical presentation and Eviatar Golan for the AFM imaging of the PVA films (Supporting Information, Figure S1).

Keywords: interfaces · monolayers · solid-phase synthesis · surface functionalization · surface patterning

How to cite: *Angew. Chem. Int. Ed.* **2016**, *55*, 12366–12371
Angew. Chem. **2016**, *128*, 12554–12559

[1] a) J. Sagiv, *J. Am. Chem. Soc.* **1980**, *102*, 92–98; b) R. Maoz, J. Sagiv, *J. Colloid Interface Sci.* **1984**, *100*, 465–496; c) R. Maoz, S. Matlis, E. DiMasi, B. M. Ocko, J. Sagiv, *Nature* **1996**, *384*, 150–153; d) K. Wen, R. Maoz, H. Cohen, J. Sagiv, A. Gibaud, A. Desert, B. M. Ocko, *ACS Nano* **2008**, *2*, 579–599.

[2] a) P. Fontaine, D. Goguenheim, D. Deresmes, D. Vuillaume, M. Garet, F. Rondelez, *Appl. Phys. Lett.* **1993**, *62*, 2256–2258; b) A. N. Parikh, M. A. Schivley, E. Koo, K. Seshadri, D. Aurentz, K. Mueller, D. L. Allara, *J. Am. Chem. Soc.* **1997**, *119*, 3135–3143; c) Y. Wang, M. Lieberman, *Langmuir* **2003**, *19*, 1159–1167; d) T. Koga, M. Morita, H. Ishida, H. Yakabe, S. Sasaki, O. Sakata, H. Otsuka, A. Takahara, *Langmuir* **2005**, *21*, 905–910; e) S. Onclin, B. J. Ravoo, D. N. Reinhoudt, *Angew. Chem. Int. Ed.* **2005**, *44*, 6282–6304; *Angew. Chem.* **2005**, *117*, 6438–6462; f) J.-R. Li, K. L. Lusker, J.-J. Yu, J. C. Garno, *ACS Nano* **2009**, *3*, 2023–2035; g) V. V. Naik, R. Städler, N. D. Spencer, *Langmuir* **2014**, *30*, 14824–14831; h) A. L. Brownfield, C. P. Causey, T. J. Mullen, *J. Phys. Chem. C* **2015**, *119*, 12455–12463.

[3] a) P. K. Bhattacharya, A. Reisman, M. C. Chen, *J. Electron. Mater.* **1988**, *17*, 273–283; b) R. J. Kinzig, *J. Electron. Mater.* **1991**, *20*, 681–686; c) C. Hordequin, D. Tromson, A. Brambilla, P. Bergonzo, F. Foulon, *J. Appl. Phys.* **2001**, *90*, 2533–2537.

[4] a) R. Maoz, E. Frydman, S. R. Cohen, J. Sagiv, *Adv. Mater.* **2000**, *12*, 725–731; b) S. Hoeppener, R. Maoz, J. Sagiv, *Nano Lett.*

2003, *3*, 761 – 767; c) S. Liu, R. Maoz, J. Sagiv, *Nano Lett.* **2004**, *4*, 845 – 851; d) D. Wouters, R. Willems, S. Hoeppener, C. F. J. Flipse, U. S. Schubert, *Adv. Funct. Mater.* **2005**, *15*, 938 – 944; e) Z. Zheng, M. Yang, B. Zhang, *J. Phys. Chem. C* **2010**, *114*, 19220 – 19226.

[5] a) A. Zeira, D. Chowdhury, R. Maoz, J. Sagiv, *ACS Nano* **2008**, *2*, 2554 – 2568; b) A. Zeira, J. Berson, I. Feldman, R. Maoz, J. Sagiv, *Langmuir* **2011**, *27*, 8562 – 8575.

[6] J. Berson, D. Burshtain, A. Zeira, A. Yoffe, R. Maoz, J. Sagiv, *Nat. Mater.* **2015**, *14*, 613 – 621.

[7] a) M. Calleja, M. Tello, R. Garcia, *J. Appl. Phys.* **2002**, *92*, 5539 – 5542; b) J. A. Dagata, F. Perez-Murano, C. Martin, H. Kuramochi, H. Yokoyama, *J. Appl. Phys.* **2004**, *96*, 2393 – 2399; c) M. Cavallini, P. Mei, F. Biscarini, R. Garcia, *Appl. Phys. Lett.* **2003**, *83*, 5286 – 5288; d) R. Garcia, A. W. Knoll, E. Rideo, *Nat. Nanotechnol.* **2014**, *9*, 577 – 587.

[8] a) E. L. Smith, C. A. Alves, J. W. Anderegg, M. D. Porter, L. M. Siperko, *Langmuir* **1992**, *8*, 2707 – 2714; b) O. Gershevitz, A. Osnis, C. N. Sukenik, *Isr. J. Chem.* **2005**, *45*, 321 – 336.

[9] R. Maoz, J. Sagiv, D. Degenhardt, H. Möhwald, P. Quint, *Supramol. Sci.* **1995**, *2*, 9 – 24.

[10] S. Akhter, K. Allan, D. Buchanan, J. A. Cook, A. Campion, J. M. White, *Appl. Surf. Sci.* **1988/1989**, *35*, 241 – 258.

[11] The spontaneous formation of ester linkages involving a fraction of the interfacial PVA hydroxyls and OTSox carboxylic acid groups generated upon irradiation (see the Experimental Section) also contributes to the drop in the intensity of the O–H stretch band.

[12] L. Li, Y.-J. Zhu, *J. Colloid Interface Sci.* **2006**, *303*, 415 – 418.

[13] Carrying out the electrical stamping in a humid atmosphere like that employed in the water-mediated patterning with Ag/OTS/Si stamps[5b] was found to yield blurred pattern features, most probably because of lateral spreading of current passing through a thin water layer that forms under such conditions at the PVA-OTS interface. Addition of water is thus detrimental to the present dry-film-mediated patterning processes.

[14] Catalytic processes adapted to surface patterning via different variants of microcontact printing have been reported in a number of publications; see, for example: a) X.-M. Li, M. Péter, J. Huskens, D. N. Reinhoudt, *Nano Lett.* **2003**, *3*, 1449 – 1453; b) J. M. Spruell, B. A. Sheriff, D. I. Rozkiewicz, W. R. Dichtel, R. D. Rohde, D. N. Reinhoudt, J. F. Stoddart, J. R. Heath, *Angew. Chem. Int. Ed.* **2008**, *47*, 9927 – 9932; *Angew. Chem.* **2008**, *120*, 10075 – 10080; c) H. Mizuno, J. M. Buriak, *J. Am. Chem. Soc.* **2008**, *130*, 17656 – 17657; d) C. Wendeln, O. Roling, C. Schulz, C. Hentschel, B. J. Ravoo, *Langmuir* **2013**, *29*, 2692 – 2699.

Received: May 20, 2016
Revised: July 29, 2016
Published online: September 5, 2016

